Northumbria
University
NEWCASTLE

Low frequency sound absorption and transmission loss performances of perforated corrugated sandwich panels provided by additive manufacturing

H. Meng[1,2,3*], M. A. Galland[2], M. Ichchou[3], O. Bareille[3], F. X. Xin[1] and T. J. Lu[1]

[1]MOE Key Laboratory for Multifunctional Materials and Structures, Xi'an Jiaotong University, Xi'an 710049, P.R. China

[2] Univ Lyon, École Centrale de Lyon, Laboratoire de Mécanique des Fluides et d'Acoustique, UMR CNRS 5509, F-69134, Écully, France

[3] Laboratoire de Tribologie et Dynamique des Systèmes, École Centrale de Lyon,36, Avenue Guy de Collongues, 69130 Ecully Cedex, France

Abstract

This paper presents numerical and experimental investigations on the low frequency sound absorption coefficient (SAC) and sound transmission loss (STL) of corrugated sandwich panels with various perforation configurations. Considered configurations includ perforations in the face plates, in the corrugated core and in both the face plates and corrugated cores. Finite element (FE) models are built up for the calculations with considerations of the acoustic-structure interactions and viscous and thermal consumptions inside the perforate pores. The numerical models are then verified by comparing with the experimental results measured in an impedance tube. Compared with the classical corrugated sandwich panels without perforations, the corrugated sandwich panels with perforated pores in the face plates can not only provide higher SAC at low frequencies, the enlargement of SAC will produce better STL at low frequencies as a consequence.. Influences of perforated pore diameter and porosity on the vibroacoustic performances are also explored. For corrugated sandwich panel with uniform perforations, resonance frequencies and bandwidths in the SAC and STL curves decreases with the increase of pore diameter and decrease of

[*]Corresponding authors.
E-mail: menghan1989.123@gmail.com (H. Meng)

porosity. Non-uniform perforations in the corrugated sandwich panels can make up for the deficiency of the uniform perforations by enlarging the bandwidth and lowering the resonance frequency.

Key words: corrugated sandwich panels, low frequencies SAC, low frequencies STL, perforations, additive manufacturing

Introduction

Sound transmission loss and absorption of panels are the two biggest acoustic issues for investigators in this area in the past decades. The most appealing structures for the sound transmission are sandwich panels made of multiple-layer panels and core structures. Sandwich structures have low density, high stiffness-to-mass ratio, and excellent thermal and acoustic characteristics, hence widely applied as soundproof concepts. Many kinds of cores exist for the sandwich panels, such as air cavity core, foams, honeycomb structures, corrugated structures and other isotropic and anisotropic cores. Extensive investigations have been dedicated to the STL of sandwich panels, and those investigations can be classified by the core types.

A great deal of investigators presented their methods for the double wall partitions with air cavity [1-7], for example, Wang *et al*. [1] predicted the STL of double leaf with air sandwich panel numerically by statistical energy analysis approach, Xin *et al*. [3] investigated analytically the STL of simply supported finite double leaf panels with enclosed air cavity. Besides, numerous studies have considered the double wall sandwich panels with sound absorbing cores instead of air cavity [8-18], for example, Bolton *et al*. [13, 17] presented calculations of STL of double-panel structures lined with elastic porous material by applying the Biot's theory for the porous material, Doutres and Atalla [12] proposed a theory to estimate the STL of double panel structure with multilayered absorbing blanket core. Sandwich panels with sound absorbing cores turned out to improve the STL at resonance frequencies. Honeycomb sandwich panels are more widely used in applications than sandwich panels with air or absorbing cores because of good mechanical efficiency, many investigators have studied the STL of honeycomb sandwich panels [19-24]. Jung *et al*. [22] presented a theory to predict STL of honeycomb sandwich panels by assuming the core is homogeneous orthotropic. Griese *et al*. [23] numerically calculated the STL performance of honeycomb sandwich panels and analyzed the effect of honeycomb core geometry on the STL of honeycomb sandwich panel. Zhou and Crocker [20] presented STL calculations of foam-filled honeycomb sandwich panel by statistical energy analysis. Rajaram *et al*. [24] investigated panel design parameters on the STL of the honeycomb sandwich panels. Tang *et al*. [21] presented a model for the estimation of STL of cylindrical sandwich shell with honeycomb core. Among all the sandwich panels, corrugated sandwich panels are the most appealing alternative in the transportation industry due to its excellent mechanical performance with limited thickness, simple configuration, structural stability and easy manufacture procedure. Shen *et al*. [25] and Xin *et al*. [26, 27] presented analytical investigations of corrugated sandwich panels by modelling the corrugated cores as translational and rotational springs. Even though the success applications of sandwich panels for settling the STL, sandwich panels are incapable for the sound absorption.

On the contrary, micro-perforated panels (MPPs) can provide effective sound absorption performances. MPPs are usually comprised of plates with submillimeter pores, an air cavity and rigid wall. Sound absorption mechanism of the MPPs is connected to Helmholtz resonance like absorption. Compared with the traditional sound absorbing materials, MPPs are more environment-friendly and suitable for severe situations, such as high temperature and high pressure. The SAC of the MPPs has been widely addressed by many investigators. Maa first [28-30] proposed an analysis model for the SAC of single and double MPPs by the electroacoustic analogy method. Atalla and Sgard [31], Allard and Atalla [32] tried to figure out the SAC of the MPPs by employing rigid frame porous material models, Beranek and Ver [33] presented a theoretical model that similar to Atalla and Sgard’s with a different correction length for the impedance. Rao and Munjal [34] and Lee and Kwon [35] used an empirical impedance model to estimate the SAC of MPPs. Despite of the efficiency in SAC, MPPs are invalid structures for the STL. Studies by Chen [36] and

Dupont *et al*. [37] showed that the SAC of the MPPs is smaller than that of single plate of the same thickness.

Nowadays, combinations of MPP and sandwich structures come into the view of researchers concerning both the STL and SAC of panels. Perforated pores in the face plates of the sandwich panels can provide effective sound absorption as MPP layers, while the backed plates and core structures can act as sound insulation barriers. Dupont *et al*. [37] first investigated the acoustic properties of a MPP coupling with a flexible plate both analytically and experimentally, they found the coupled MPP-air cavity-plate system could increase the STL while maintaining a good SAC. To improve the STL at mid frequencies, Toyoda and Takahashi [38] subdivided the air cavity of the MPP-air cavity-plate system by inserting honeycomb structures to the air cavity. Bravo *et al*. [39, 40] proposed a fully coupled model approach to calculate the SAC and STL of single or multi-layer MPPs and plates, and results showed that SAC and STL at resonance frequencies were controlled by the relative velocities of air-frame and the MPP-back panel. Mu *et al*. [41] added MPP layer both to the source and transmitted side of double leaf panels and found the MPP layer weakened the mass-air-mass resonance.

These investigations concern the acoustical properties of sandwich panels with face plate perforations. The middle cores of these sandwich panels are air gap or honeycomb structures. None of these investigations considers corrugated sandwich panels with perforations. Corrugated sandwich panels are an appealing structure for STL in application. Different from the honeycomb sandwich panels, corrugated sandwich panels can have perforations in the corrugated pores as well as in the face plates (see Fig. 1). It will be interesting for investigators in this area to see the new SAC and STL by various perforation configurations in corrugated sandwich panels.

However, the perforations in the corrugated sandwich panels are micro-sized that makes the manufacture of perforated sandwich panels extremely difficult by conventional manufacturing methods. Hence, the additive manufacturing (also known as 3D printing) is employed to fabricate the perforated corrugated sandwich panels. In an additive manufacturing progress, the expected structures are created by laying down thin layers of materials according to the digital CAD models. Nowadays, many kinds of 3D printers occur, including direct metal laser sintering (DMLS), selective laser melting (SLM), fused deposition modeling (FDM), etc. [42]. These different 3D printers can create objects from many materials, plastics, sandstones, porcelains, pure metals, alloys and almost everything in-between. The additive manufacturing can not only print structures with elaborate shapes, it is also a more time-saving method than conventional manufacturing methods.

Therefore, this paper deals with the SAC and STL of corrugated sandwich panels with perforations at normal incidence. Section 1 presents FE models to calculate the SAC and STL of corrugated sandwich panels with different perforation configurations. Section 2 describes an experiment conducted in an impedance tube for the validation of the FE models. Based on the FE models proposed in section 1, section 3 compares the SAC and STL of corrugated sandwich panels with different perforation configurations. The influences of the perforated pore diameter and porosity are also discussed in section4.

1. Corrugated sandwich panels with perforations by FE models

Figure 1 shows 4 kinds of corrugated sandwich panels with different perforation configurations. The sample in Fig. 1(a) represents classical corrugated sandwich panels without perforation. The wall thicknesses of the two face plates and corrugated core are h_1, h_2 and t respectively. The distance between the two plates is H. The inclination angle of the corrugated core is φ, and the width of the unit cell of the corrugated core is L .Samples in Figs. 1(b)(c)(d) have perforated pores of submillimeter~ millimeter scale in the upper face plates, corrugated cores and both the two places respectively. The diameters of perforated pores in the face plate and the corrugated core are d_1 and d_2 respectively. It is noted that for all these corrugated sandwich panels, no perforated pores exist on the lower face plate to achieve more effective STL.

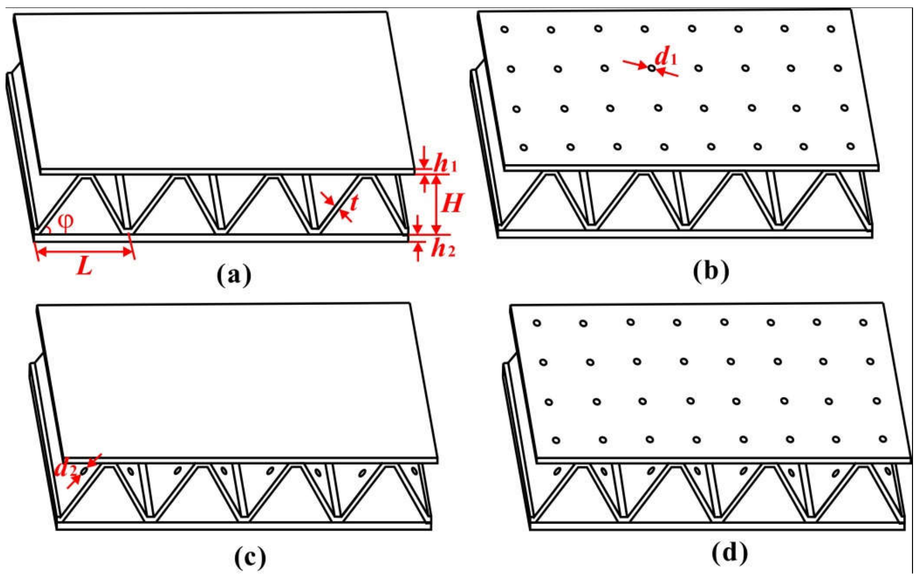

Fig. 1 Schematic of classical corrugated sandwich panel and corrugated sandwich panels with various perforation configurations

When a plane wave impinges on the upper face plate, the acoustical properties of the corrugated sandwich panels can be calculated by the FE model shown in Fig. 2. The FE model is set up by using the software COMSOL Multiphysics. The plane wave is applied to the incidence field. Two Perfectly Match layers (PML) are added to the incident and transmitted field to simulate infinite and non-reflecting domain.

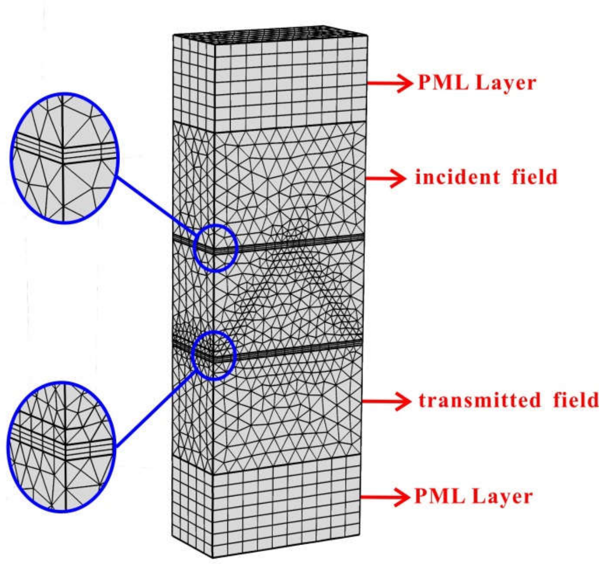

Fig.2 Numerical model of a unit cell of the corrugated sandwich panel

The air in the incident, transmitted and middle field is compressible but lossless flow, with no thermal conductivity and viscosity considered. Thus the pressure field model, which is suited for all frequency-domain simulations with harmonic variations of the pressure field, is applied. The sound pressure in these fields is governed by Helmholtz equation:

$$\nabla^2 p = \frac{1}{c_0^2}\frac{\partial^2 p}{\partial t^2} \tag{1}$$

where p is the sound pressure, t is the time and c_0 is the sound speed.

The solid components of the structures are isotropic linear elastic materials during the simulation, Solid Mechanics module is applied for the vibration of the solid panels, the displacement of the panel is governed by

$$-\rho\omega^2\mathbf{u} - \frac{1}{2}\nabla\cdot\left((\nabla\mathbf{u})^{\mathrm{T}} + \nabla\mathbf{u}\right) = Fe^{-i\omega t} \tag{2}$$

where $\mathbf{u}$ represents the displacement of the solid panels, ρ is the density of the solid panel, ω is angular frequency, and F represents the total sound pressure exerted on the solid panel.

As to the air inside the small pores, the radius of pores is of comparable size with the thermal boundary thickness and viscous boundary thickness at low frequencies, which means the thermal conduction and viscosity should be considered during the simulation, therefore, thermal-acoustic modulus is applied, the sound pressure, temperature, and particle velocity is governed by three equation, the linear Navier-Stokes equation, mass continuity equation and thermal conduction equation, given as below:

$$\begin{aligned}
&i\omega\rho_0\mathbf{v} = \nabla\cdot\left(-p + \eta\left(\nabla\mathbf{v} + (\nabla\mathbf{v})^{\mathrm{T}}\right) - \frac{2}{3}\eta\nabla\cdot\mathbf{v}\right)\\
&i\omega\rho_0\left(\frac{p}{P_0} - \frac{T}{T_0}\right) + \rho_0\nabla\cdot\mathbf{v} = 0\\
&i\omega\rho_0 C_p T = -\nabla\cdot(-K\nabla T) + i\omega p
\end{aligned} \tag{3}$$

where $\mathbf{v}$ is fluid velocity, and T is temperature variation, ρ_0 is the density of air, η is the dynamic viscosity. C_p denotes the heat capacity of air at constant pressure, K is thermal conductivity. Besides, P_0 and T_0 represent equilibrium pressure and temperature.

For the corrugated sandwich panels of infinite size, FE simulations can be conducted by a unit cell with periodic boundary condition as shown in Fig. 2. While for panels of finite size, the whole panels with actual boundaries should be embodies in FE models. Model settings for the air and solid frame mentioned before are applicable for both infinite and finite sized samples.

The sound energy E is divided into three parts during propagation through the composite panel:

$$E = E_{ref} + E_{trans} + E_{absorp} \tag{4}$$

where E_{ref} denote the reflected sound energy in the incident field, E_{trans} denotes the transmitted sound energy in the transmitted sound field, while E_{absorp} denotes the absorbed energy inside the sandwich panel. E_{ref} is calculated by:

$$E_{ref} = \frac{1}{2}\mathrm{Re}\int_S \left\{ \left(\mathbf{p}_1 - \mathbf{p}_i\right) \cdot \left(-\mathbf{v}_1 + \mathbf{v}_i\right)^* \right\} dS \tag{5}$$

where $\mathbf{p}_1$ and $\mathbf{v}_1$ are the sound pressure and velocity at the surface of the top face plate in the incident field, $\mathbf{p}_i$ and $\mathbf{v}_i$ are the sound pressure and velocity of the incident plane wave.

The transmitted energy E_{trans} is given as:

$$E_{ref} = \frac{1}{2}\mathrm{Re}\int_S \mathbf{p}_3 \cdot \mathbf{v}_3^* dS \tag{6}$$

where $\mathbf{p}_3$ and $\mathbf{v}_3$ are the sound pressure and velocity at the surface of the bottom face plate in the transmitted field. Hence, the STL can be given as:

$$\mathrm{STL} = 10\log_{10}\frac{E}{E_{trans}} \tag{7}$$

The SAC is written as:

$$\alpha = 1 - \frac{E_{trans}}{E} - \frac{E_{ref}}{E} \tag{8}$$

2. Experimental validation

Experimental measurements were performed to validate the FE models by using the four microphones B & K standing wave tube with the two load method shown in Fig. 3. A loudspeaker mounted at the end of the tube was set to generate a random signal over the frequency range 100~1600 Hz. 4 microphones were installed at the four measuring position to measure the complex sound pressures. Note the tubes with a diameter of 100 mm were chosen, which is suitable for low frequency measurement 100~1600 Hz. A transfer matrix method was applied to obtain the acoustic properties of the tested samples developed by Bolton *et al.*[43]. The transfer matrix elements were solved by two independent measurements which were conducted with open tube termination and reverberant termination respectively. The reverberant termination was created with 3 standard samples with an approximately 75 mm depth in total.

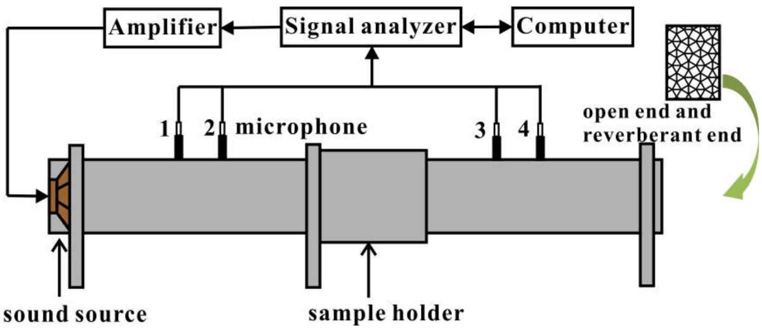

Fig. 3 Schematic of the experimental system

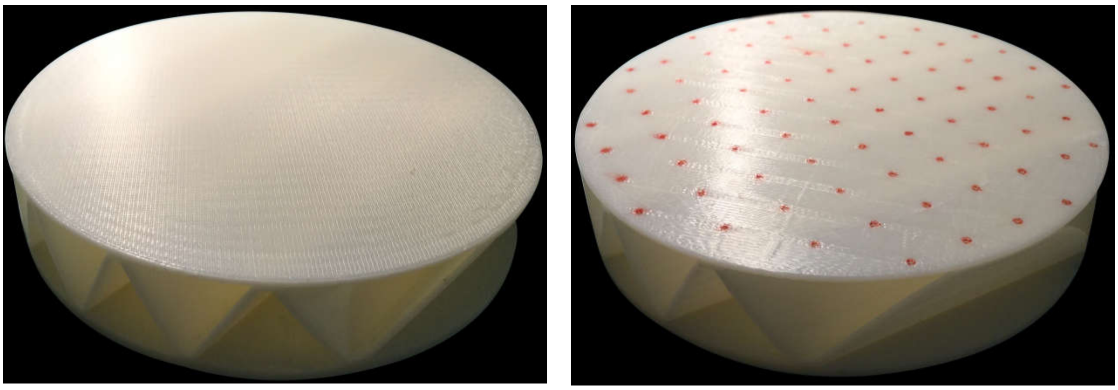

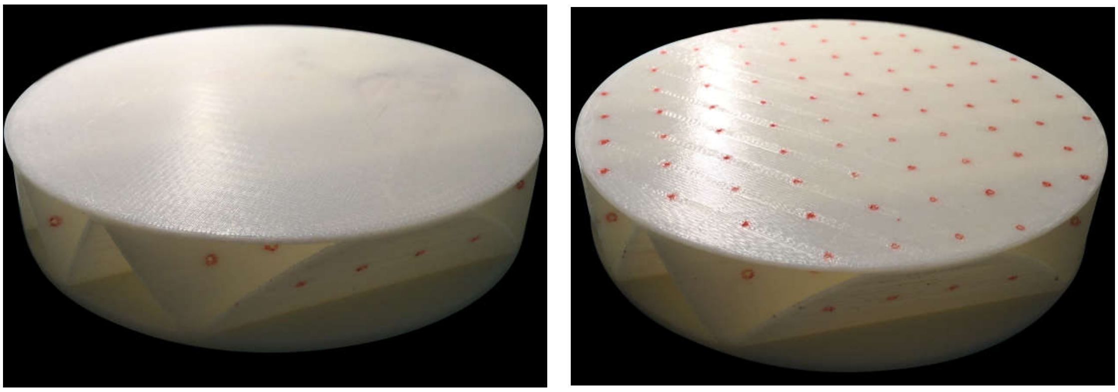

Fig. 4 Corrugated sandwich panel samples for impedance tube test

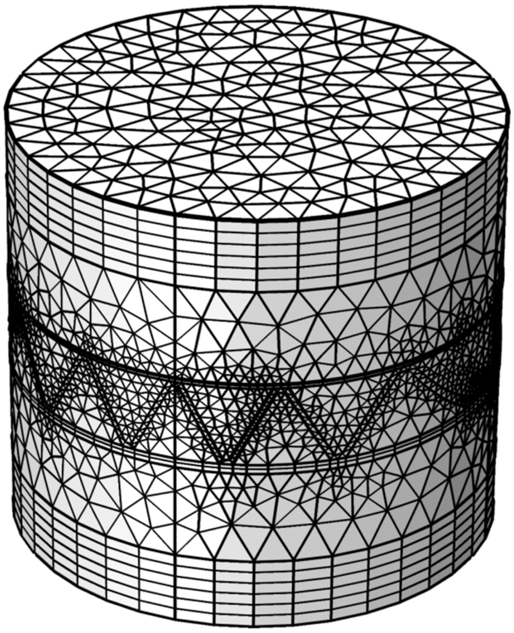

Fig. 5 FEM models for samples for test

Figure 4 shows the four tested samples corresponding to the four types of panels in Fig. 1. The samples were manufactured by a FDM 3D printer with a density of 958 kg/m^3, Young’s modulus 1 GPa and Poisson’ ratio of 0.35. The geometrical parameters of the samples are shown in Table 1. During the measurement, the samples were fixed in the tube. FE models of finite size with fixed boundary conditions identical to the experimental conditions are set up (see Fig. 5) by applying the FE method in the last section.

Table 1 Geometrical parameters of the corrugated sandwich panels samples in experiment

Parameters	Value

face plates thicknesses	$h_1 = 1$ mm $h_2 = 2$ mm
distance between face plates	$H = 17$ mm
perforation ratios	$\sigma_1 = \sigma_2 = 0.78\%$
pores diameters	$d_1 = d_2 = 1$ mm
wall thickness of the core	$t = 1$ mm
inclination angle of the core	$\varphi = 63.4°$
unit cell width of the core	$L = 20$ mm

The tested STLs are compared with that by simulation in Fig. 6. The tested STLs agree well with the simulation results for all these samples, which proves that the FE methods presented are effective to estimate the acoustical properties of the corrugated sandwich panels. The deviations at low frequencies are mainly introduced by the non-ideal experimental conditions and manufacturing errors of samples.

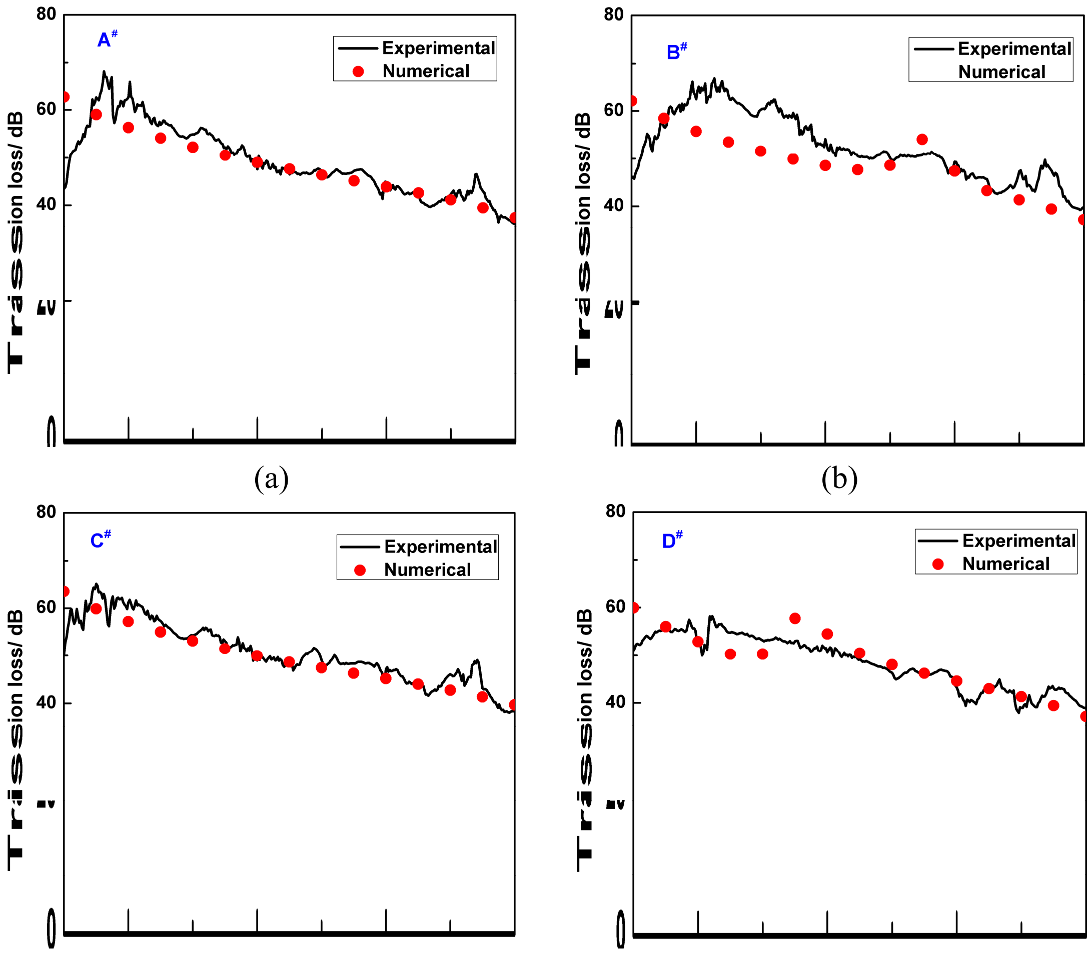

(a) (b)

(c) (d)

Figure 6 Comparison between the STL by FEM and experimental measurement

3. Results and Discussion

3.1 Influence of perforation configurations

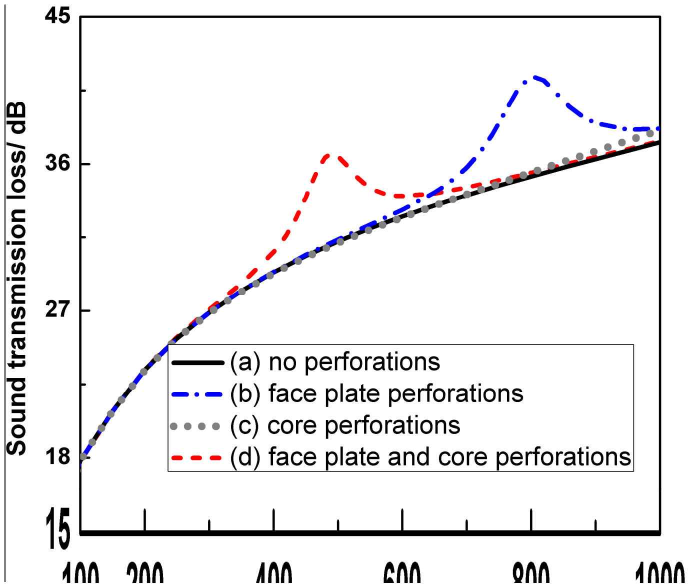

Fig.7 STL comparison among corrugated sandwich panels with different perforation configurations

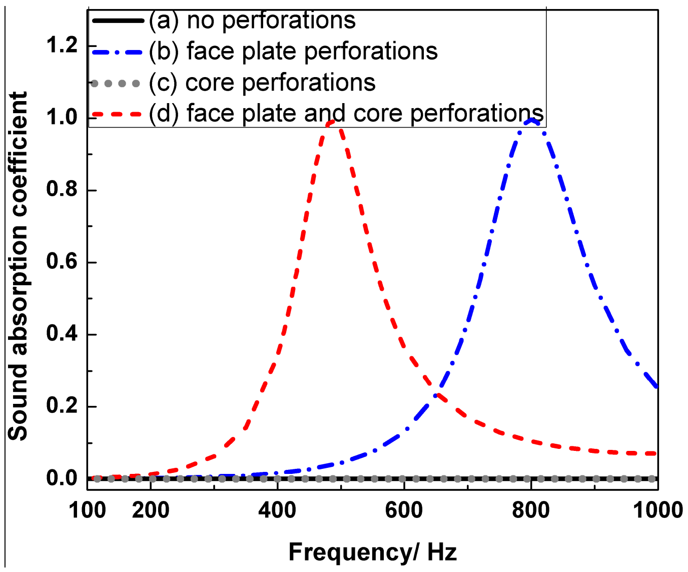

Fig.8 SAC comparison among corrugated sandwich panels with different perforation configurations

Based on the previous FE models proposed, this section compares the STL and SAC of the four kinds of corrugated sandwich panels. For simplification, sandwich panels of infinite size are considered. These panels are assumed fabricated by aluminum with a density of 2700 kg/m^3, Young's modulus of 70 GPa, and Poisson's ratio of 0.33.

Table 2 Geometrical parameters of the calculated corrugated sandwich panels

Parameters	**Value**
face plates thicknesses	$h_1 = h_2 = 1$ mm
distance between face plates	$H = 18$ mm
perforation ratios	σ_1=σ_2=0.349%
pores diameters	$d_1 = d_2 = 1$ mm
thickness of the core	$t = 1$ mm
inclination angle of the core	φ=54.8°
unit cell width of the core	$L = 30$ mm

The STL and SAC of the classical corrugated sandwich panel and corrugated sandwich panels with various perforation configurations are compared in Fig. 7 and Fig. 8. The geometrical parameters of the corrugated sandwich panels are listed in Table 2. It can be seen from Figs. 7 and 8 that compared with classical corrugated sandwich panels without perforation, sandwich panels with perforations in the face plate have better SAC and STL at low frequencies, while the sandwich panels with perforations only in the corrugated core have almost identical STL and SAC curves. For sandwich panels with face plate perforations, the sound waves can enter into the small pores during the propagation. The SAC can be dramatically enlarged since the sound energy will be consumed by the viscous and thermal effects inside the small pores. Due to the improvement of absorbed energy, the transmitted energy will be reduced, which will bring out increment of STL. On the contrary, for sandwich panels with perforation in the corrugated cores, most of the sound energy will be reflected by the upper face plate, therefore, the SAC is negligibly small, simultaneously, no improvement occurs in the STL. Besides, it also can be seen that resonance frequencies exist in the SAC and STL curves of corrugated sandwich panels with face plate perforations. Sandwich panels with perforations in both the face plate and middle core have lower resonance frequency than that with only face plate perforations.

It can be concluded that the perforations have great influence in the STL and SAC of corrugated sandwich panels. Sandwich panels with perforations both in the face plate and cores have the best acoustic properties at low frequencies. Hence, further study of the perforations will be conducted based on the corrugated sandwich panels with both face plate and core perforations. Influences of pore diameters and pore size will be discussed in the following section.

3.2 Influence of pore diameter

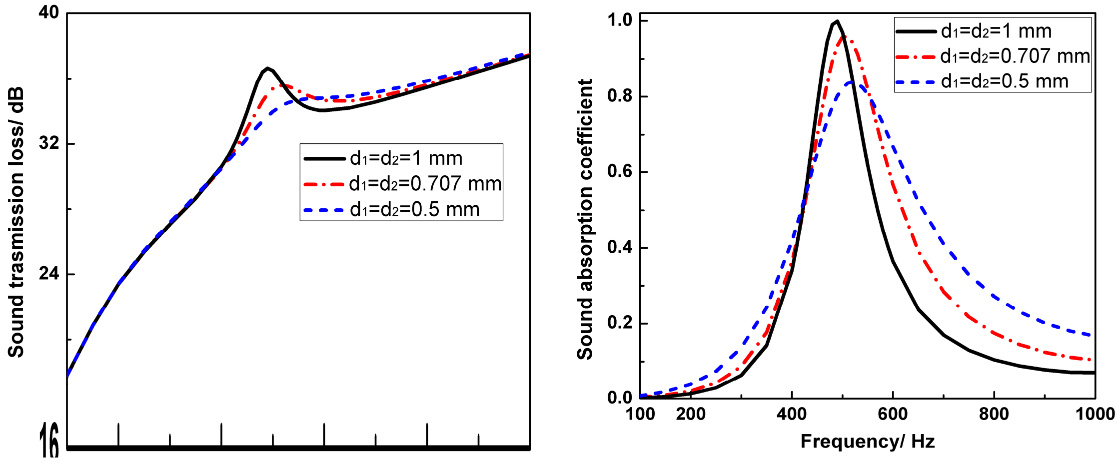

Fig.9 STL and SAC comparison among corrugated sandwich panels with perforations of different pore diameters

Figure 9 compares the STL and SAC of three corrugated sandwich panels with same geometrical parameters (as listed in Table 2) apart from the perforated pore diameters. For all the three sandwich panels, the pore diameters are uniformly distributed, namely, the diameter of pores in the face plates is equal to that in the corrugated cores of the same corrugated sandwich panels. It can be seen from Fig. 9 that with the decrease of the pore diameter, the bandwidth of SAC increases. When the porosity is fixed, the air-fluid interface area inside the perforated pores increases with the decrease of pore diameter. The improved air-fluid interface area will increase the acoustic resistance, which will enlarge the bandwidth in SAC and STL as a consequence. It also can be seen from Fig. 9 that the decrease of pore diameter can enlarge the resonance frequencies and reduce the peak values in STL and SAC curves. Corrugated sandwich panels are ideally expected to have high peak values, big bandwidths and low resonance frequencies in SAC and STL curves at the same time. However, obviously, there exists a contradiction between increment of bandwidth and decrease of resonance frequencies and increment of peak values for sandwich panels with uniform pore diameters. Therefore, corrugated sandwich panels with non-uniform pore diameters are resorted to balance this problem as shown in Fig. 10.

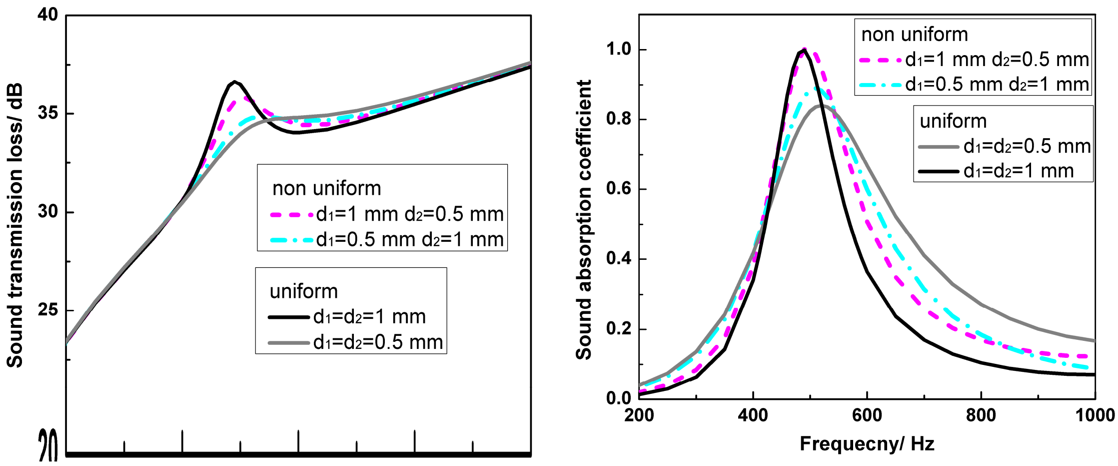

Fig.10 STL and SAC comparison among corrugated sandwich panels with perforations of uniform and non-uniform pore diameters

Figure 10 compares the STL and SAC of the sandwich panels with uniform and non-uniform perforated pore diameters. For the two non-uniformly perforated sandwich panels, diameters of pores in the face plate are different from that in the corrugated core of the same panel, instead, the pore diameters of the two places are in descending and ascending orders respectively. It can be seen from Fig. 10 that the non-uniform pore diameters in the sandwich panels can remedy defects introduced by uniform pores. The non-uniformly perforated sandwich panels have bigger bandwidth than the uniformly perforated sandwich panels with bigger pore diameter, and higher peak value and lower resonance frequency than uniformly perforated sandwich panels with smaller pore diameter. In addition, Fig 10 also shows that sandwich panels with non-uniform pores diameters in descending order have better STL and SAC at low frequencies than that in ascending order.

3.3 Influence of porosity

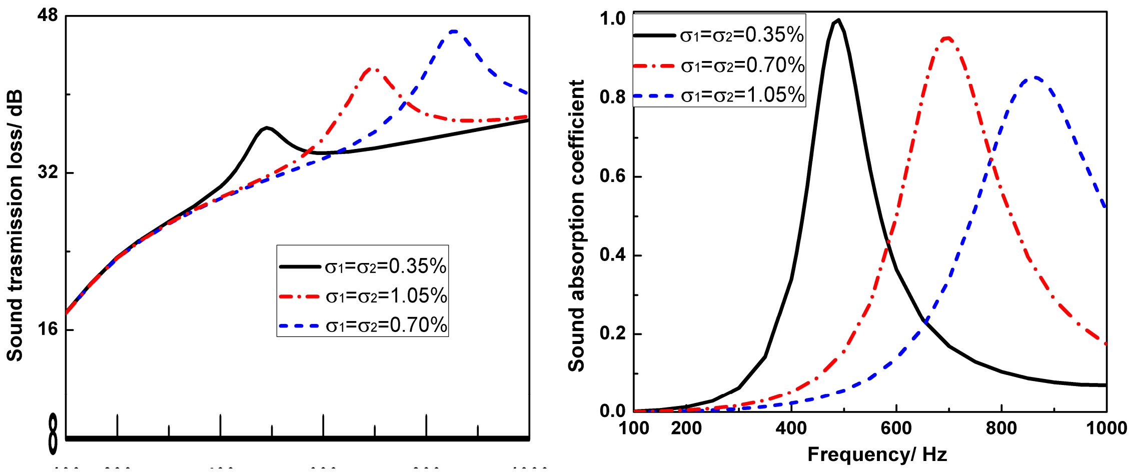

Fig.11 STL and SAC comparison among corrugated sandwich panels with perforations of different porosities

This subsection discusses the influence of perforated porosity on the STL and SAC of the corrugated sandwich panels. The perforated corrugated sandwich panels have the same geometrical parameters (as listed in Table 2) except porosities. Note that for the three sandwich panels discussed in Fig. 11, the porosity of pores in the face plate is identical with that in the corrugated cores of the same sandwich panel. It can be seen from Fig. 11 that the bandwidth improves with the increase of porosity, which can be also attributed to the increment of acoustic resistance by enlarged porosity. Besides, the resonance frequency decreases with the decrease of porosity. Contradiction between the decrease of resonance frequency and increase of bandwidth also exists for corrugated sandwich panels with uniform porosity. Therefore, corrugated sandwich panels with non-uniform porosities are explored in Fig. 12.

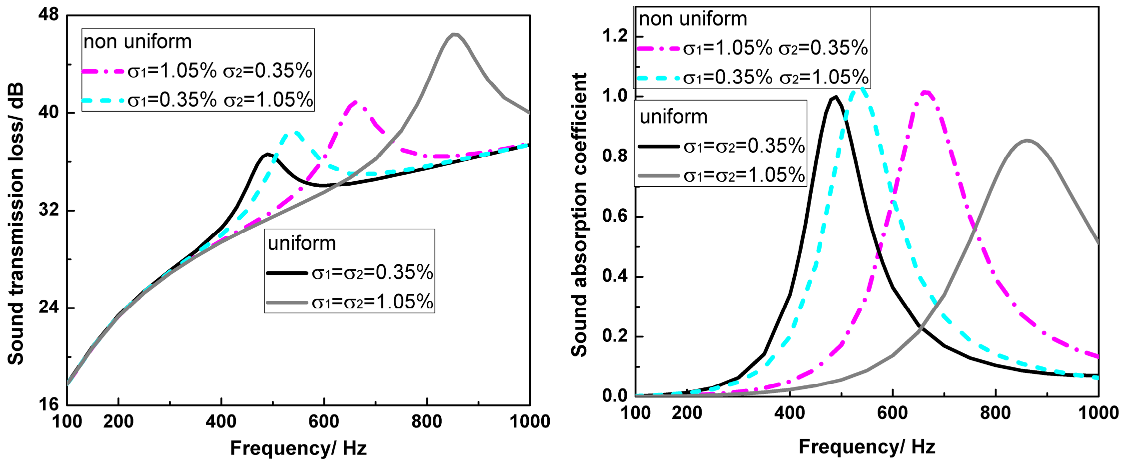

Fig.12 STL and SAC comparison among corrugated sandwich panels with perforations of uniform and non-uniform porosities

The STL and SAC of corrugated sandwich panels with non-uniform porosities are compared with that of corrugated sandwich panels with uniform porosities in Fig. 12. The pore porosities of the face plates and corrugated cores are in descending order and ascending orders respectively for corrugated sandwich panels with non-uniform porosities. It can be seen from Fig. 12 that the sandwich panels with non-uniform porosities have lower resonance frequencies than the uniformly perforated sandwich panels with relatively bigger porosity, and larger bandwidth than the uniformly perforated sandwich panels with relatively smaller porosity. Besides, it also can be seen from Fig. 12 that sandwich panels with non-uniform porosities in ascending order have better STL and SAC at low frequencies that that in descending order.

Conclusions

In this study, corrugated sandwich panels with perforations are numerically investigated from the SAC and STL viewpoint. A finite element method model is presented by applying Comsol Multiphysics. The air in the incident, middle and transmitted field is regarded as compressible inviscid flow calculated with the Pressure acoustics module. By contrast, since the diameter of the pores is comparable to the viscous and thermal boundary layer thickness, the air inside the pores is assumed as compressible viscous flow modeled withy Thermacoustics module. The rigid frames of the MPPCP are flexible structures calculated with the Solid Mechanics module. Calculated STL is then validated by comparing with experimental resulst. Afterwards, comparisons between the classical corrugated sandwich panels and corrugated sandwich panels with face plate perforations prove the face plate perforations are effective to improve the SAC and STL at low frequencies. Meanwhile, the resonance frequencies and bandwidths in SAC and STL curves are shown to decrease with the increase of pore diameter and decrease of porosity. Corrugated sandwich panels with non-uniform perforated pore diameters or porosities can have better SAC and STL than that with uniform pore dimeters and porosities at low frequencies. Results obtained in the present paper can help researchers to design superior structures that aim at reducing both reflection and transmission with internal noise. Further optimization work can be conducted based on the corrugated sandwich panels with non-uniform perforations.

Acknowledgement

Reference

[1] T. Wang, S. Li, S. Rajaram, S.R. Nutt, Predicting the Sound Transmission Loss of Sandwich Panels by Statistical Energy Analysis Approach, J Vib Acoust, 132: 011004-011007.

[2] A. London, Transmission of reverberant sound through double walls, J Acoust Soc Am, 22 (1950) 270-279.

[3] F.X. Xin, T.J. Lu, C.Q. Chen, Sound transmission through simply supported finite double-panel partitions with enclosed air cavity, J Vib Acoust, 132 (2010) 011008: 011001-011011.

[4] A.J. Price, M.J. Crocker, Sound transmission through double panels using statistical energy analysis, J Acoust Soc Am, 47 (1970) 683-693.

[5] J.D. Chazot, J.L. Guyader, Prediction of transmission loss of double panels with a patch-mobility method, J Acoust Soc Am, 121 (2007) 267-278.

[6] R.J.M. Craik, Non-resonant sound transmission through double walls using statistical energy analysis, Appl Acoust, 64 (2003) 325-341.

[7] F.X. Xin, T.J. Lu, Analytical and experimental investigation on transmission loss of clamped double panels: Implication of boundary effects, J Acoust Soc Am, 125 (2009) 1506-1517.
[8] A. Cummings, K.A. Mulholland, The transmission loss of finite sized double panels in a random incidence sound field, J Sound Vib, 8 (1968) 126-133.
[9] K. Mulholland, H. Parbrook, A. Cummings, The transmission loss of double panels, J Sound Vib, 6 (1967) 324-334.
[10] L.L. Beranek, G.A. Work, Sound transmission through multiple structures containing flexible blankets, J Acoust Soc Am, 21 (1949) 419-428.
[11] J.-D. Chazot, J.-L. Guyader, Transmission loss of double panels filled with porogranular materials, J Acoust Soc Am, 126 (2009) 3040-3048.
[12] D. Olivier, A. Noureddine, Acoustic contributions of a sound absorbing blanket placed in a double panel structure: Absorption versus transmission, J Acoust Soc Am, 128 664-671.
[13] J. Bolton, E. Green, Normal incidence sound transmission through double-panel systems lined with relatively stiff, partially reticulated polyurethane foam, Appl Acoust, 39 (1993) 23-51.
[14] R. Panneton, N. Atalla, Numerical prediction of sound transmission through finite multilayer systems with poroelastic materials, J Acoust Soc Am, 100 (1996) 346-354.
[15] Y.J. Kang, J.S. Bolton, A finite element model for sound transmission through foam-lined double-panel structures, J Acoust Soc Am, 99 (1996) 2755-2765.
[16] A. Trochidis, A. Kalaroutis, Sound transmission through double partitions with cavity absorption, J Sound Vib, 107 (1986) 321-327.
[17] J.S. Bolton, N.M. Shiau, Y.J. Kang, Sound transmission through multi-panel structures lined with elastic porous materials, J Sound Vib, 191 (1996) 317-347.
[18] W.C. Tang, H. Zheng, C.F. Ng, Low frequency sound transmission through close-fitting finite sandwich panels, Appl Acoust, 55 (1998) 13-30.
[19] T.A. Wang, V.S. Sokolinsky, S. Rajaram, S.R. Nutt, Assessment of sandwich models for the prediction of sound transmission loss in unidirectional sandwich

panels, Appl Acoust, 66 (2005) 245-262.

[20] R. Zhou, M.J. Crocker, Sound transmission loss of foam-filled honeycomb sandwich panels using statistical energy analysis and theoretical and measured dynamic properties, J Sound Vib, 329 (2010) 673-686.

[21] Y.Y. Tang, J.H. Robinson, R.J. Silcox, Sound transmission through a cylindrical sandwich shell with honeycomb core, 34th AIAA aerospace science meeting and exhibit, 1996, pp. 877-886.

[22] J.-D. Jung, S.-Y. Hong, J.-H. Song, H.-W. Kwon, A Study on Transmission Loss Characteristics of Honeycomb Panel for Offshore Structures, J Appl Math Phys, 3 (2015) 172.

[23] D. Griese, J.D. Summers, L. Thompson, The Effect of Honeycomb Core Geometry on the Sound Transmission Performance of Sandwich Panels, J Vib Acoust, 137 (2015) 021011.

[24] S. Rajaram, T. Wang, S. Nutt, Sound transmission loss of honeycomb sandwich panels, Noise Contr Eng J, 54 (2006).

[25] C. Shen, F. Xin, T. Lu, Theoretical model for sound transmission through finite sandwich structures with corrugated core, Int J Nonlinear Mech, 47 (2012) 1066-1072.

[26] F.X. Xin, T.J. Lu, Effects of Core Topology on Sound Insulation Performance of Lightweight All-Metallic Sandwich Panels, Mater Manuf Process, 26 (2011) 1213-1221.

[27] F.X. Xin, T.J. Lu, C. Q. Chen, Sound transmission through lightweight metallic sandwich panel with corrugated core, Acta Acustica, 4 (2008) 010.

[28] D.-Y. Maa, Theory and design of microperfoated panel sound-absorbing constructions, Sci China (1975).

[29] D.-Y. Maa, Wide band sound absorber based on microperforated panels, Chin J Acoust, 3 (1985).

[30] D.-Y. Maa, Potential of microperforated panel absorber, J Acoust Soc Am, 104 (1998) 2861-2866.

[31] [31] N. Atalla, F. Sgard, Modeling of perforated plates and screens using rigid

frame porous models, J Sound Vib, 303 (2007) 195-208.

[32] J.F. Allard, N. Atalla, *Propagation of Sound in Porous Media: Modelling Sound Absorbing Materials 2e*, Wiley, 2009.

[33] L.L. Beranek, I.L. Vér, *Noise and Vibration Control Engineering: Principles*, Wiley, 1992.

[34] K.N. Rao, M. Munjal, Experimental evaluation of impedance of perforates with grazing flow, J Sound Vib, 108 (1986) 283-295.

[35] D.H. Lee, Y.P. Kwon, Estimation of the absorption performance of multiple layer perforated panel systems by transfer matrix method, J Sound Vib, 278 (2004) 847-860.

[36] K.-T. Chen, Study on the acoustic transmission loss of a rigid perforated screen, Appl Acoust, 47 (1996) 303-318.

[37] T. Dupont, G. Pavic, B. Laulagnet, Acoustic properties of lightweight micro-perforated plate systems, Acta Acust, 89 (2003) 201-212.

[38] M. Toyoda, D. Takahashi, Sound transmission through a microperforated-panel structure with subdivided air cavities, J Acoust Soc Am, 124 (2008) 3594-3603.

[39] T. Bravo, C. Maury, C. Pinhède, Sound absorption and transmission through flexible micro-perforated panels backed by an air layer and a thin plate, J Acoust Soc Am, 131 (2012) 3853-3863.

[40] T. Bravo, C. Maury, C. Pinhède, Enhancing sound absorption and transmission through flexible multi-layer micro-perforated structures, J Acoust Soc Am, 134 (2013) 3663-3673.

[41] R.L. Mu, M. Toyoda, D. Takahashi, Sound insulation characteristics of multi-layer structures with a microperforated panel, Appl Acoust, 72 (2011) 849-855.

[42] B.P. Conner, G.P. Manogharan, A.N. Martof, L.M. Rodomsky, C.M. Rodomsky, D.C. Jordan, J.W. Limperos, Making sense of 3-D printing: Creating a map of additive manufacturing products and services, Addit Manuf 1 (2014) 64-76

[43] Bolton, J. S., Yoo, T. & Olivieri, O. Measurement of normal incidence transmission loss and other acoustical properties of materials placed in a standing

wave tube. Brüel & Kjær Tech Rev, (2007)1-44.